An Isotope Edited Classical Raman Difference Spectroscopic Study of the Interactions of Guanine Nucleotides with Elongation Factor Tu and H-*ras* p21†

Danny Manor,‡ Gezhi Weng,‡ Hua Deng,‡ Sharon Cosloy,§ Cun-xiang Chen,∥ Valeria Balogh-Nair,∥ Kathy Delaria,⊥ Frances Jurnak,⊥ and Robert Callender*,‡

Departments of Physics, Biology, and Chemistry, City College of the City University of New York, New York, New York 10031, and Department of Biochemistry, University of California at Riverside, Riverside, California 92521

Received June 14, 1991; Revised Manuscript Received August 26, 1991

ABSTRACT: We have measured the Raman spectrum of GDP bound to the elongation factor protein, EF-Tu, and the c-Harvey-*ras* protein, p21, two proteins of the guanine nucleotide binding family. In order to separate the Raman spectrum of the nucleotide from the much more intense protein spectrum, we investigate the feasibility of "tagging" the normal modes of the nucleotide by isotopic substitution, here by incoporating deuterium-labeled guanine at the C8 position into the active site. A difference spectrum between the labeled and unlabeled protein–nucleotide complex shows the changes in the Raman spectrum of the bound nucleotide that arise from the isotopic exchange. We find that surprisingly good Raman spectra of bound ligands can be obtained with this method and that the method can be easily generalized to other systems. The data show that the guanine amino group of the nucleotide interacts differently with both EF-Tu and p21 than it does with water, showing a change in hydrogen-bonding properties upon binding. On the other hand, no change in hydrogen bonding is observed at guanine's N7. The data strongly suggest that the conformation of the nucleotide when bound to EF-Tu and that p21 is the C2′ endo pucker of the ribose ring and anti about the glycosidic bond. These results are compared to previous structural and chemical studies.

A number of key biochemical pathways are regulated in vivo by a family of guanine nucleotide binding proteins. These proteins, which have been shown to play crucial roles in such diverse pathways as protein biosynthesis, sensory transduction, and malignant transformation, share strong functional and structural homologies [for reviews see Bourne et al. (1990, 1991), Masters et al. (1986), and Wooley and Clark, (1989)]. Physiologically, they are all complexed with one equivalent of either GDP or GTP, and their biochemical activity is tightly regulated by the nature of the bound ligand. In general, guanine nucleotide binding proteins are biologically "active" when complexed with GTP, which is hydrolyzed during catalysis to yield the "silent" GDP-complexed form. GDP is exchanged for GTP with the aid of an activating factor.

We report here on two proteins within this class using vibrational spectroscopy. One, EF-Tu,[1] is an elongation factor in prokaryotic protein biosynthesis; it is responsible for transporting and coupling aminoacyl-tRNAs (aa-tRNA) to the ribosome where they are added to the nascent peptide chain. EF-Tu–GTP binds aa-tRNA and ribosomes with high affinity, both of which increase the internal GTPase activity of the protein, yielding EF-Tu–GDP, which dissociates from the ribosome. The cycle is started when the bound GDP is exchanged for GTP by elongation factor Ts (Kaziro, 1978). p21 proteins are products of the protooncogenic *ras* genes which are found in most mammalian cells, and their point mutated forms are prevalent in many human tumors (Barbacid, 1987). Although little is known regarding the biochemical nature of p21 action, it is generally expected that p21–GTP exerts a signal which somehow induces cell growth and proliferation. The p21–GTP protein exhibits GTPase activity, which is further enhanced by the GAP protein (Adari et al., 1988; Cales et al., 1988; Trahey & McCormick, 1987). This yields the p21–GDP product which is a "quiet", nonsignaling complex. The point-mutated oncogenic p21 proteins generally exhibit substantially slower GTPase activity. GDP is exchanged for GTP with the aid of recently discovered releasing factors (Downward et al., 1990). It is thus of considerable interest to explore the interactions between the bound nucleotides and these proteins.

Vibrational spectroscopy provides a wealth of information on the conformations and structures of molecules, particularly small molecules, as well as protein–ligand interactions, like hydrogen bonding which perturbs a molecule's electronic distribution. In this latter case, the modified electronic distribution results in modified vibrational force constants, sometimes along quite well defined and important coordinates. Thus, the changes observed in the vibrational spectra of a bound ligand are a direct measure of how a protein acts upon it. An important experimental constraint, however, in the use of vibrational spectroscopy has been that the signals from proteins are generally much greater than those of bound ligand. The signals from a bound ligand, or other small molecular

† This work was supported in part by Grant DMB-8912322 (R.C., V.B.-N., S.C.) from The National Science Foundation and by Grants EYO3142 (R.C.) and GM26895 (F.J.) from The National Institutes of Health.

‡ Department of Physics, City College of the City University of New York.

§ Department of Biology, City College of the City University of New York.

∥ Department of Chemistry, City College of the City University of New York.

⊥ Department of Biochemistry, University of California at Riverside.

[1] Abbreviations: p21, gene product of the human c-H-*ras* protooncogene; EF-Tu, elongation factor Tu from *E. coli*; GD(T)P, guanosine 5′-di(tri)phosphate; Tris, tris(hydroxymethyl)aminomethane; DTE, 1,4-dithioerythritol; PMSF, phenylmethanesulfonyl fluoride; EDTA, (ethylenedinitrilo)tetraacetic acid; GAP, GTPase activating protein; SDS-PAGE, SDS–polyacrylamide gel electrophoresis; RP-HPLC, reverse-phase high-performance liquid chromatography; ORD, optical rotary dispersion; CD, circular dichroism.

0006-2960/91/0430-10914$02.50/0

protein moieties, are difficult to isolate. One approach in overcoming this difficulty is to employ resonance Raman spectroscopy [cf. Spiro (1987, 1988)]. In this case, the exciting laser light is in resonance with a chromophore, and this yields greatly increased Raman cross-sections. A number of very important chromophoric protein systems have been so studied. Unfortunately, this approach is limited to proteins which contain spectrally isolated chromophores.

We have succeeded previously in describing complex formation between enzymes, their substrates, and cofactors in a family of dehydrogenases [cf. Chen et al. (1987), Deng et al. (1989c), and Yue et al. (1989, 1984)], to a level of quantitating hydrogen-bonding patterns (Deng et al., 1989a) and in situ protonation states (Deng et al., 1989b; Yue et al., 1991), using ultrasensitive non-resonance Raman difference techniques. This report summarizes our initial efforts in applying, and enlarging, these techniques to EF-Tu and p21 as representatives of the GTPase superfamily. In our earlier studies, the non-resonance Raman spectrum of the enzyme–substrate complex was measured as was that of the enzyme itself. The difference spectrum between these two is obtained, and it contains bands which arise from the bound substrate as well as protein bands which arise from protein changes induced by substrate binding. This procedure cannot be used here because EF-Tu and p21 are unstable without a bound ligand. We therefore have taken a somewhat different approach in this study. The bound nucleotide is replaced by (a stable) isotopically labeled nucleotide, and the spectra of the protein–nucleotide and protein–(labeled) nucleotide are taken. The difference spectrum formed between these two then arises from modes which are affected ("edited") by the label, and all other parts of the Raman difference spectrum subtract to zero.

We report first our results on the Raman spectra of EF-Tu and p21 containing GDP. We then discuss and characterize the difference spectra obtained between unlabeled and labeled protein–GDP complexes. For these first measurements, we have incorporated GDP where the C8 hydrogen of the guanine group (8D-GDP) has been replaced by a deuterium. Many guanine bands are affected by this substitution so that the difference spectrum contains a number of bands which characterize quite well the vibrational properties of guanine. The difference spectrum of GDP's guanine moiety in EF-Tu and p21 is obtained with remarkably high signal to noise (over 30 to 1 for the largest band). This suggests that this form of spectroscopy may be used in a number of studies where the properties of bound ligands are of interest. The study performed here may be generalized to proteins of any size (at least in principle), to proteins in solution, or to membrane-bound proteins.

Materials and Methods

Chemicals. GDP was from Aldrich or Boehinger Mannheim. All other chemicals were from the highest purity available. [^{3}H]GDP (12 Ci/mmol) was from Amersham. 8D-GDP ([8-^{2}H]GDP) was prepared from unlabeled GDP in the presence of phosphate by a modification of published methods (Shelton & Clark, 1967; Tsang et al., 1987). A total of 10 mg of nucleotide was dissolved in 1 mL of D_2O in the presence of 20–25 mg of Na_2DPO_4. The mixture was stirred at 90 °C for 5 h and was then evaporated to dryness and resuspended in H_2O four times. More than 97% of the 8-position was deuterated and was stable in H_2O for more than a week according to ^{1}H NMR. The phosphate and contaminating nucleotide monophosphates were then removed by passing the sample through a P-2 column (Bio-Rad, Richmond, CA; 1.5 cm × 35 cm, in H_2O).

Proteins. EF-Tu–GDP was prepared from *Escherichia coli* MRE 600 (Grain Processing Corp., Muscatine, IA) as described (Louie et al., 1984). p21–GDP was purified from *E. coli* strain RRIDM15 containing the ptac-c-H-*ras* plasmid according to Tucker et al. (1986). Both proteins were >95% pure as judged by SDS–PAGE. All preparations were analyzed for their nucleotide content by RP-HPLC (Darwish & Prichard, 1981; John et al., 1990). Purified proteins were stored at −70 °C in buffer A (50 mM Tris-HCl, pH 7.6, 10 mM $MgCl_2$, 0.5 mM DTE, 1 mM NaN_3, 0.1 mM PMSF) containing 0.1 mM GDP. Prior to the Raman experiment, proteins were concentrated to ~2 mM (EF-Tu) or ~4 mM (p21) in buffer R (10 mM $MgCl_2$, 20 mM sodium phosphate, pH 7.6) using a Centricon centrifugal concentrator (Model 30 for EF-Tu and Model 10 for p21; Amicon Corp., Beverly, MA). Proteins remained fully active during and after the Raman experiment, as determined by the [^{3}H]GDP binding assay (Miller & Weissbach, 1974). Protein concentrations were determined spectroscopically using molar extinction coefficients (280 nm) of 40 000 M^{-1} cm^{-1} for EF-Tu (Miller & Weissbach, 1974) and 18 450 M^{-1} cm^{-1} for p21 (Tucker et al., 1986), or by the Lowry method (Bradford, 1976).

Preparation of 8D-Nucleotide Complexes. Protein samples (300 μL, ca. 1 mM) were incubated with a 10-fold molar excess of 8D-GDP in buffer A for 30 min at 37 °C. For p21, the incubation mixture included 50 mM K_2SO_4 and 0.6 mM EDTA, and $MgCl_2$ was added to 1 mM before the next step. The samples were then diluted with 2 mL of cold buffer R and concentrated to 100 μL as above. The incubation with 8D-GDP was repeated once more, and the samples were washed with buffer R five more times to yield ~60 μL, at 2–4 mM, for the Raman experiment. This procedure ensured nearly 100% replacement of the bound GDP with less than 0.2% nucleotide remaining free in solution.

Spectroscopy. Raman spectra were measured with an optical multichannel array system consisting of a Triplemate spectrometer (Spex Industries, Metuchen, NJ) and a solid-state detector system (Model DIDA-1000 water-cooled photodiode array and a Model ST-100 detector controller; Princeton Instruments, Trenton, NJ). Data were acquired, stored, and analyzed on a Mac-II computer (Apple, Cupertino, CA). A detailed description of the Raman difference spectrometer has been given previously (Deng et al., 1989c; Yue et al., 1989). A total of 150 mW of the 488-nm line from a Coherent INOVA-200 argon ion laser (Coherent Radiation Inc., Palo Alto, CA) was used for the Raman excitation of EF-Tu and free nucleotides, and 150 mW of 530.1 nm from a Coherent 2000-CR krypton ion laser was used for p21. Fluorescent background observed in p21 spectra was decreased by keeping the sample for 2 h in the laser light prior to data collection. Spectral lines were calibrated against known Raman lines of toluene and are accurate to within 3 cm^{-1}. Spectral resolution is ±8 cm^{-1}.

Results and Discussion

The classical Raman spectra of the GDP-bound proteins are shown in parts a (EF-Tu) and c (p21) of Figure 1. A few initial notes are worth mentioning on the quality of the data. We have found the non-resonance Raman signals of the most intense guanine bands to be on the order of 3% of the 1449-cm^{-1} protein band of proteins having a molecular weight of ca. 40 000, like EF-Tu. This is a convenient marker band because it arises from a CH_2 scissoring mode which is fairly insensitive to environment. This small difference is quite difficult to detect by a simple visual examination of the data.

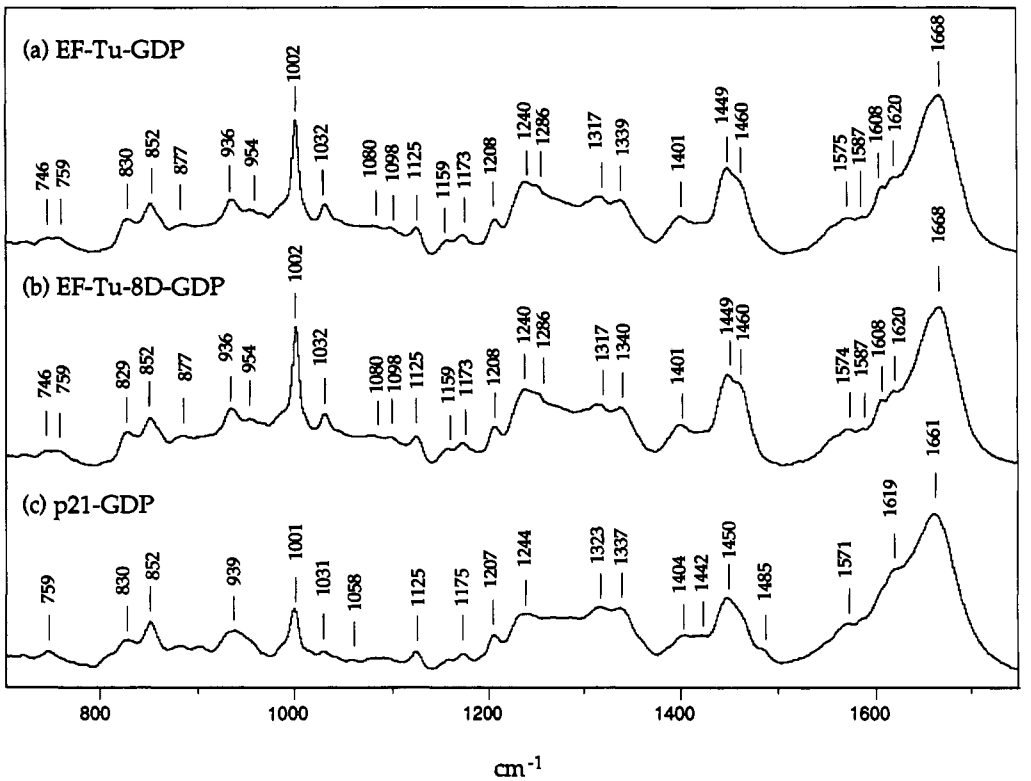

FIGURE 1: Raman spectra of (a) EF-Tu–GDP, (b) EF-Tu–8D-GDP, and (c) p21-GDP. EF-Tu–GDP is at 2 mM in buffer R and is excited with 180 mW of 488-nm argon laser light. p21-GDP is at 3.6 mM in buffer R and is excited with 150 mW of 530.2-nm krypton laser light.

For example, the substitution of a deuteron at guanine's C8 position markedly affects the Raman spectrum of the nucleotide (see below). However, the combined Raman spectrum of EF-Tu with bound 8D-GDP in Figure 1b "looks" virtually identical to that with bound 8H-GDP shown in Figure 1a. These differences are only revealed by sensitive and reliable difference techniques, as shown below. A minimal requirement for an adequate measurement of bound guanine by difference spectroscopy is that the measured protein signals achieve a signal to noise ratio of much better than 30/1. We have found EF-Tu to be one of the more suitable proteins for Raman studies that we have encountered so far in this regard. The purification procedures for this protein work very well with regard to fluorescing impurities (we expect no fluorescence from the protein because the visible excitation used to stimulate the Raman light is far from any protein absorption band). EF-Tu yields virtually no background fluorescence. Moreover, it is easy to prepare in high concentrations (~2 mM) with no aggregation. We have not determined the signal to noise in the EF-Tu data partly because the channel resolution along the frequency axis is not sufficiently fine. However, the signal to noise of the data in Figure 1a exceeds 1000/1. On the other hand, p21 does show some background fluorescence levels, and the signal to noise ratio for the data of Figure 1b is somewhat less, near 300/1. This results in a somewhat more noisy difference spectrum for p21 than for EF-Tu (see below). We are in the process of finding an additional purification step that will eliminate this problem for future studies. In addition, we observed a nonreversible change of the Raman spectrum when p21 was highly concentrated (>6 mM).

Protein Structure. Because the Raman spectra of proteins were shown to represent the spectral sum of its constituent amino acids (Lord & Tu, 1970), most Raman peaks in parts a and c of Figure 1 can be assigned to their corresponding residues as is shown in Table I. Except for minor position changes, all amino acids that are present in both proteins show similar frequency and intensity patterns.

Table I: Raman Peak Frequencies and Mode Assignments for the GDP-Bound Forms of EF-Tu (Left) and p21 (Parentheses) Proteins[a]

Raman frequency (cm^{-1})	assignment	Raman frequency (cm^{-1})	assignment
643 (-)	Tyr	1207 (1207)	Phe, Tyr
825 (830)	Tyr (buried)	1200–1300	amide III
850 (850)	Tyr (exposed)	1317 (1320)	C–H def
936 (938)	Val, CH_3 sym rock	1338 (1339)	C–H def
950 (951)	C–C str	1400 (1407)	COO^-, str, Asp, Glu
1001 (1002)	Phe		
1030 (1030)	Phe	1449 (1450)	CH_2 sc
-(1059)	C–N str	1571 (1570)	?
1124 (1124)	C–N str	1605 (-)	Phe, Tyr
1172 (1174)	Phe, Tyr, Val, Leu, CH_3 asym rock	1618 (1618)	Phe, Tyr, Trp
		1667 (1663)	amide I

[a] Taken from the spectra shown in Figure 1. Abbreviations: str, stretching; def, deformation; sc, scissoring. Assignments are based on Otto et al. (1987) and Thomas and Prescott (1976, 1983), and references cited therein.

Nucleotide Spectroscopy. There have been a number of previous Raman studies of nucleotides and isotopically substituted derivatives (Benevides et al., 1984; Delabar & Majoube, 1978; Lane & Thomas, 1979; Majoube, 1984, 1985; Mathlouthi et al,. 1986; Nishmura et al., 1986a; Peticolas et al., 1987; Tsuboi et al., 1973, 1987). However, we show solution data of GDP and 8D-GDP (Lane & Thomas, 1979) in Figure 2 for reference, and we follow the previous rather detailed spectral assignments in our discussion below (Lane & Thomas, 1979; Majoube, 1984; Mathlouthi et al., 1986; Tsuboi et al., 1987). The spectrum of GDP is dominated by bands which are associated with the guanine residue. The substitution of a deuterium at the C8 position of guanine affects the frequencies of a number of bands. The strongest band at 1485 cm^{-1}, which has been assigned to ring stretch

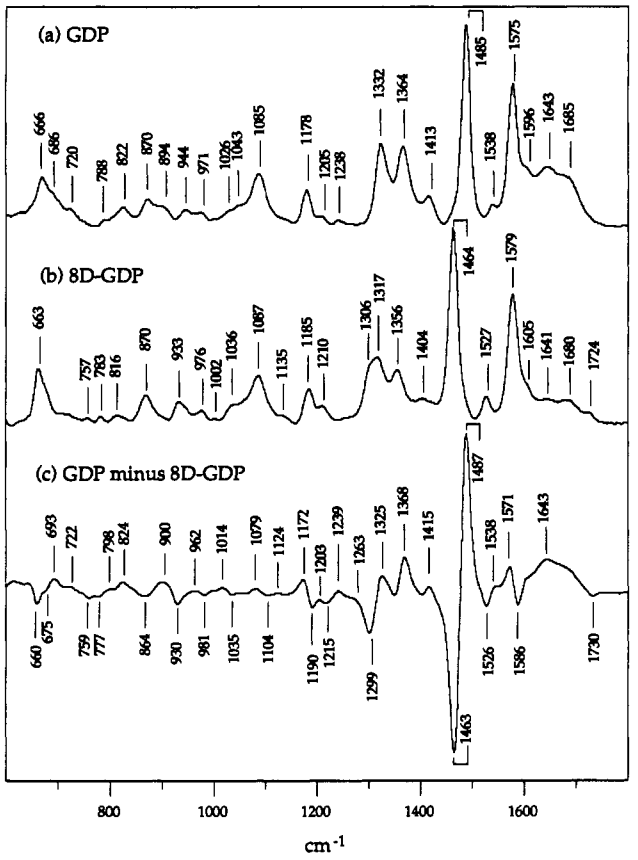

FIGURE 2: Raman spectra of (a) GDP and (b) 8D-GDP and (c) the calculated difference spectrum. Both samples are at 50 mM in H_2O, pH 7.5. Excitation is with 100 mW of 488-nm argon laser light.

and 8-CH deformation, shifts down nearly 20 cm^{-1} to 1464 cm^{-1} in the 8D-GDP data. This band shifts substantially to lower frequency upon complexation with heavy ions or hydrogen bonding to guanine's N7 (Nishimura et al., 1986b). Bands that show up in the Raman spectrum of guanosine from 1300 to 1400 cm^{-1} arise from ring motions and contain as well as substantial motions from the bonded ribose group. The pattern of bands in this range, their positions, and their intensities, as well as of those in the 600–700-cm^{-1} range, are quite sensitive to the torsional angle about the glycosidic bond and the pucker state of the ribose ring. Tsuboi and his colleagues (Nishimura et al., 1986b) have determined the Raman spectra of a number of guanosine (and cytidine) salts have compared their Raman spectra with the guanosine conformations determined by X-ray diffraction analysis. The pattern of the bands in the 600–700- and 1300–1400-cm^{-1} regions of the solution spectra of Figure 1a most closely follows crystal spectra where the guanosine conformation is C2′ endo–anti. It has been proposed that the peak at 1178 cm^{-1} is sensitive to hydrogen bonding to guanine's $-NH_2$ group. This mode is believed to be composed of guanine ring plus C–N (amino) stretch. Thus, variations in hydrogen bonding to the amino group, which would be expected to influence the C–N stretch, may be reflected in this mode's frequency. Peticolas and his co-workers interpreted a 5-cm^{-1} downward shift in this band upon warming poly(G) from 25 to 90 °C as the breaking of hydrogen bonds to this group (Small & Peticolas, 1971). The band at 1085 cm^{-1} arises principally from motions on the phosphate (P–O stretch) part of GDP. Underneath this band is a small peak which has been assigned to motions on the ribose group.

As discussed above, our procedure for measurement of the Raman spectrum of the bound nucleotide involved isotopically "editing" the in situ nucleotide and forming the Raman difference spectrum between the labeled and unlabeled protein–ligand complex. Figure 2c shows the difference spectrum between Raman spectra of GDP (Figure 2a) and 8D-GDP (Figure 2b). This difference spectrum has been obtained by our difference spectrometer as described under Materials and Methods and in previous reports (Deng et al., 1989c; Yue et al., 1989). Essentially, a measurement of the GDP spectrum is taken as well as one of the 8D-GDP spectrum. The spectra are stored in the computer and are then digitally subtracted. Our current accuracy in this procedure is a subtraction fidelity of 0.1% (Yue et al., 1989). All normal modes which include the C8-H coordinate are affected by deuteration of the 8-position, and these show as positive and negative peaks in the difference spectrum. For example, the strongest band in the GDP spectrum (1485 cm^{-1}), assigned to stretching vibration of the N7=C8 bond and 8-CH deformation, is shifted to 1464 cm^{-1}, giving rise to the derivative-like feature dominating the difference spectrum. Most of the guanine bands found in the GDP spectrum are affected by the substitution of deuterium at C8, and this results in a complex and rich difference spectrum.

The zero crossings are of importance in a difference spectrum. Assuming that a particular band can be described by a Lorentzian intensity profile centered at ν_u (for unlabeled) and that the band shifts by $\Delta\nu$ to ν_l (for labeled) upon labeling without change in intensity or bandwidth, then the intensity profile for the unlabeled band is

$$I_u = \frac{A}{(\nu - \nu_u)^2 + 1/4\Gamma^2}$$

where the profile for the labeled band is

$$I_l = \frac{A}{(\nu - \nu_l)^2 + 1/4\Gamma^2}$$

where Γ is the bandwidth and A is an intensity scaling constant. It can be easily calculated[2] that the difference between I_u and I_l goes to zero at the average frequency position, $(\nu_u + \nu_l)/2$, regardless of the bandwidth and frequency shift. Thus, for example, the 1178-cm^{-1} band in the GDP spectrum shifts to 1185 cm^{-1} in the 8D-GDP spectrum. The positive and negative "couple" that this yields in the difference spectrum is found at 1172 and 1190 cm^{-1}, respectively. The average of 1178 and 1185 cm^{-1} at 1181.5 cm^{-1} corresponds well to the 1181.0-cm^{-1} zero crossing in the difference spectrum. This relation will be used below to find the average "position" of a band of the bound GDP data.

On the other hand, it is clear that some information is lost in forming a difference spectrum. Of course, bands not associated with the substitution, like the 1085-cm^{-1} phosphate band, subtract out and are not observed. Additionally, it is sometimes difficult, without knowing the answer, to make a clear-cut association between a positive and negative "pair" in the difference spectrum and a band in the GDP spectrum and its associated shifted band in the 8D-GDP spectrum. For example, the 666-cm^{-1} GDP band shifts to 663 cm^{-1} in 8D-GDP. However, there are other nearby bands which shift differently. The result is a negative band at 660 cm^{-1} in the difference spectrum without a clearly identifiable corresponding positive peak.

GDP Bound to EF-Tu and p21. Figure 3a shows the difference spectrum of EF-Tu–GDP (Figure 1a) with that of

[2] This relation can be shown to hold for any symmetric (even) functional form of the intensity profile.

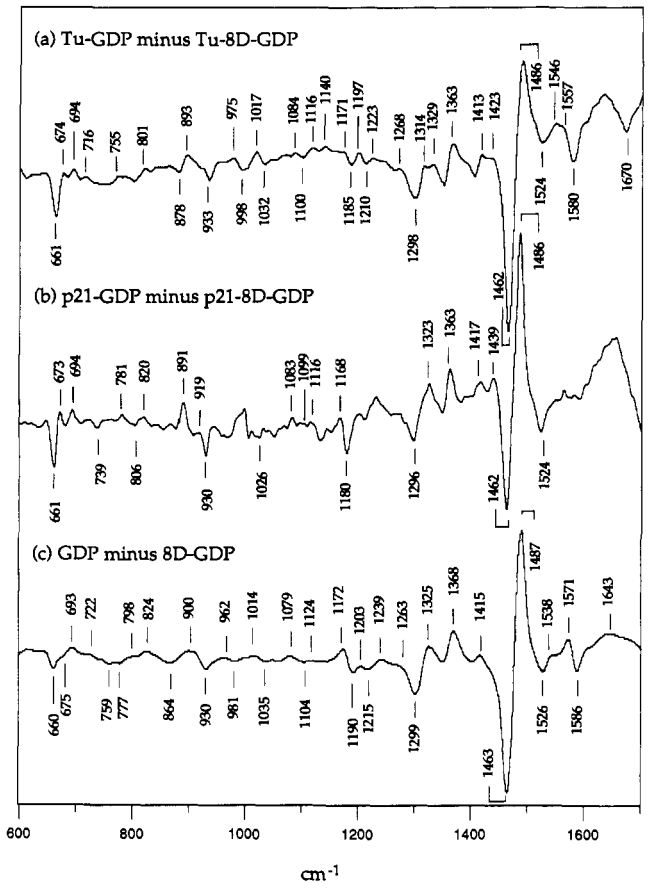

FIGURE 3: Difference spectra between the GDP and 8D-GDP complexes with (a) EF-Tu and (b) p21. Spectrum c is the solution difference spectrum (same as Figure 2c).

EF-Tu–8D-GDP (Figure 1b). The corresponding difference spectrum for the c-Harvey-*ras* p21 protein is shown in Figure 3b, and the solution difference spectrum, given in Figure 2c, is reproduced in Figure 3c for comparison. All peaks which are larger than our inherent signal to noise in these measurements and which have been observed in several independent measurements are labeled in the figure. Qualitatively, the three difference spectra are very similar. In general, the protein spectra are sharper than the solution spectrum, and the p21 spectrum is somewhat sharper than the EF-Tu spectrum. However, the peak positions are not much affected by binding.

There are several binding "handles" in GDP which have been implicated in determining the specificity of the guanine nucleotide binding site for both p21 and EF-Tu[3] [and which are generally conserved within the much larger group of GTPases; cf. Halliday (1983) and Masters et al. (1986)]. One series of interactions has to do with the phosphate groups. Interactions at this region can be divided into two: through the chelated Mg^{2+} ion (Ser-17 and Thr-35 hydroxyls in p21 and Asp-80 carboxylate in EF-Tu) and direct interactions with the phosphates. Lys-16 in p21 and Lys-24 in EF-Tu are hydrogen bonded to the phosphate oxygens, as well as a few backbone amide protons. In this study, we are unable to observe the frequencies of normal modes associated with the bound phosphates so that the effects of these interactions on the bond orders of, for example, P–O stretch, are unobservable. The incorporation of ^{18}O would shift the frequencies of these modes and make such an observation possible.

The bound data of Figure 3 clearly reflect interactions, or lack thereof, between the guanine moiety and its protein pocket. The peak at 1178 cm^{-1}, believed to be sensitive to hydrogen bonding to guanine's $-NH_2$ group (Small & Peticolas, 1971; see above), shifts to lower frequency when GDP binds to EF-Tu and p21. This is seen from the data of Figure 3 by calculating the zero intensity position of this band in the various difference spectra. In solution, the positive and negative peaks in the difference spectrum are found at 1172 and 1190 cm^{-1}, respectively. We take the zero position as the average of the positive and negative values (see above), which is 1181 cm^{-1} here. Using the same criterion, we find a zero crossing for this band at 1178 cm^{-1} from the EF-Tu data and 1174 cm^{-1} from the p21 spectrum. The band has downshifted -3 cm^{-1} for GDP in EF-Tu and -7 cm^{-1} in p21. Thus, the data suggest that guanine's amino group interacts differently with both proteins than in solution. This is consistent with binding studies (Hwang & Miller, 1987) and the available X-ray diffraction studies (de Vos et al., 1988; Jurnak, 1985; Jurnak et al., 1990; la Cour et al., 1985; Milburn et al., 1989; Pai et al., 1989; Schlichting et al., 1990a) which suggests that the guanine base is anchored by two major interactions: an aspartic acid residue (Asp-119 in p21 and Asp-138 in EF-Tu) which is hydrogen bonded with the amino substituent in position 2 and an interaction between the 6-keto group and a main-chain amine of Ala-146 in p21 and the side-chain amine of Asn-135 in EF-Tu. It should be pointed out that the correlation found previously for the 1178-cm^{-1} band suggests a decrease in frequency to be indicative of a stronger hydrogen bond. However, the mode is a fairly complicated one, and it is unclear just how it will respond to particular hydrogen-bonding groups (which is unknown in the previous work as opposed to a carboxylate here) and their positioning. These parameters may well affect the exact response of a particular mode (Latajka & Scheiner, 1990) and the sign of a shift for a complicated mode. This needs to be probed more fully with direct isotropic labeling of the amino group and model compound studies.

The data clearly indicate that the guanine ring in situ does not interact with the protein in both p21 and EF-Tu through the N7 position differently than it interacts with water in solution. This is seen from the general similarity of the bound difference data to that of the solution data. In particular, the 1486-cm^{-1} band, which is shifted by the C8 deuterium substitution to 1463 cm^{-1}, is not affected at all by binding. As discussed above, this bands has been shown to be a marker band for hydrogen bonding to N7. This conclusion is supported by the fact that modification of the 8-position with bulky groups as in 8-Br-GDP has almost no influence on the binding affinity to either EF-Tu or p21 (Eccleston et al., 1989; Wittinghofer et al., 1977).

The general correspondence in the conformationally sensitive 600–700- and 1300–1400-cm^{-1} regions between the solution spectrum and the protein spectra suggests that binding does not affect the conformation of the nucleotide. As discussed above, the solution spectrum suggests an anti conformation about the glycosidic ring and a C2′ endo sugar pucker. Thus, the data strongly suggest that the conformation of the nucleotides to EF-Tu and p21 is also C2′ endo–anti. This is in agreement with X-ray diffraction studies on these bound complexes which show a C2′ endo sugar pucker and a torsional angle of $\chi = -125°$ for GDP bound to EF-Tu and $\chi = -113°$

[3] The nucleotide–protein interactions in the following discussion are based on refined, high-resolution (1.35 Å) structural determinations for p21. The current structural resolution for EF-Tu (2.7 Å) does not allow for such conclusive statements, and the interactions are, therefore, only suggested.

for p21 in the crystalline state (de Vos et al., 1988; Jurnak, 1985; Jurnak et al., 1990; la Cour et al., 1985; Milburn et al., 1989; Pai et al., 1989; Schlichting et al., 1990a), as well as with NMR data (Schlichting et al., 1990b). It is also consistent with the crystallographic observations that the ribose of the nucleotide has only weak interactions with the protein, and a large portion of it (the 2′ and 3′ hydroxyls) is exposed to the solvent. The additional sharpness of the bands in the bound data suggests that there is less conformational accessibility for GDP bound to the proteins than when in solution. We suspect that the difference band at 661 cm^{-1} is somewhat sharper for GDP in p21 than in EF-Tu because the range of angles from an equilibrium C2′ endo ribose pucker angle is somewhat larger in EF-Tu than in p21. This conjecture, as well as the extra sharpness of the p21 spectrum compared to the EF-Tu spectrum generally, is in agreement with the somewhat greater binding affinity of p21 for GDP ($K_d = 2 \times 10^{-11}$ M; John et al., 1990) than that of EF-Tu ($K_d = 2 \times 10^{-9}$ M; Delaria & Jurnak, 1989).

ACKNOWLEDGMENTS

We thank Prof. A. Wittininghofer (Heidelberg, FRG) for his generous gift of the cloned p21 gene.

Registry No. GDP, 146-91-8.

REFERENCES

Adari, H., Lowry, D. R., Willumsen, B. M., Der, C. J., & McCormick, F. (1988) *Science 240*, 518–521.

Barbacid, M. (1987) *Annu. Rev. Biochem. 56*, 779–827.

Benevides, J. M., Lemeur, D., & Thomas, G. J. (1984) *Biopolymers 23*, 1011–1024.

Bourne, H. R., Sanders, D. A., & McCormick, F. (1990) *Nature 348*, 125–131.

Bourne, H. R., Sanders, D. A., & McCormick, F. (1991) *Nature 349*, 117–127.

Bradford, M. M. (1976) *Anal. Biochem. 72*, 248–254.

Cales, C., Hancock, J. F., Marshall, C. J., & Hall, A. (1988) *Nature 332*, 548–551.

Chen, D., Yue, K. T., Martin, C., Rhee, K. W., Sloan, D., & Callender, R. (1987) *Biochemistry 26*, 4776–4784.

Darwish, A. A., & Prichard, R. K. (1981) *J. Liq. Chromatogr. 4*, 1511–1524.

Delabar, J.-M., & Majoube, M. (1978) *Spectrochim. Acta 34A*, 129–140.

Delaria, K., & Jurnak, F. (1989) *Anal. Biochem. 177*, 188–193.

Deng, H., Zheng, J., Burgner, J., & Callender, R. (1989a) *J. Phys. Chem. 93*, 4710–4713.

Deng, H., Zheng, J., Burgner, J., & Callender, R. (1989b) *Proc. Natl. Acad. Sci. U.S.A. 86*, 4484–4488.

Deng, H., Zheng, J., Burgner, J., Sloan, D., & Callender, R. (1989c) *Biochemistry 28*, 1525–1533.

de Vos, A. M., Tong, L., Milburn, M. V., Matias, P. M., Jancarik, J., Noguchi, S., Nishimura, S., Miura, K., Ohtusuka, E., & Kim, S.-H. (1988) *Science 239*, 888–893.

Downward, J., Riehl, R., Wu, L., & Weinberg, R. A. (1990) *Proc. Natl. Acad. Sci. U.S.A. 87*, 5998–6002.

Eccleston, J. F., Kanagasabi, T. F., Molloy, D. P., Neal, S. E., & Webb, M. R. (1989) in *The Guanine Nucleotide Binding Proteins* (Bosch, L., Kraal, B., & Parmeggiani, A., Eds.) pp 87–97, Plenum Press, New York.

Halliday, K. R. (1983) *J. Cyclic Nucleotide Protein Phosphorylation Res. 9*, 435–448.

Hwang, Y.-W., & Miller, D. L. (1987) *J. Biol. Chem. 262*, 13081–13085.

John, J., Sohmen, R., Feurstein, J., Linke, R., Wittinghofer, A., & Goody, R. S. (1990) *Biochemistry 29*, 6058–6065.

Jurnak, F. (1985) *Science 230*, 32–36.

Jurnak, F., Heffron, S., Schick, B., & Delaria, K. (1990) *Biochim. Biophys. Acta 1050*, 209–214.

Kaziro, Y. (1978) *Biochim. Biophys. Acta 505*, 95–127.

la Cour, T. F. M., Nyborg, J., Thirup, S., & Clark, B. F. C. (1985) *EMBO J. 4*, 2385–2388.

Lane, M. J., & Thomas, G. J. (1979) *Biochemistry 18*, 3839–3846.

Latajka, Z., & Scheiner, S. (1990) *Chem. Phys. Lett. 174*, 179–184.

Lord, R. C., & Tu, N. T. (1970) *J. Mol. Biol. 50*, 509–524.

Louie, A., Ribeiro, S. N., Reid, B. R., & Jurnak, F. (1984) *J. Biol. Chem. 259*, 5010–5016.

Majoube, M. (1984) *J. Mol. Struct. 114*, 403–406.

Majoube, M. (1985) *Biopolymers 24*, 1075–1087.

Masters, S. B., Stroud, R. M., & Bourne, H. R. (1986) *Prot. Eng. 1*, 47–54.

Mathlouthi, M., Seurve, A., & Koenig, J. (1986) *Carbohydr. Res. 146*, 15–27.

Milburn, M. V., Tong, L., DeVos, A. M., Brunger, A. Yamaizumi, Z., Nishimura, S., & Kim, S. (1989) *Science 247*, 939–945.

Miller, D. L., & Weissbach, H. (1974) *Adv. Enzymol. Relat. Areas Mol. Biol. 30*, 219–232.

Nishimura, Y., Tsuboi, M., Sato, T., & Aoki, K. (1986a) *J. Mol. Struct. 146*, 123–153.

Nishimura, Y., Tsuboi, M., Sato, T., & Aoki, K. (1986b) *J. Mol. Struct. 146* , 123–153.

Otto, C., De Mule, F. F. M., & Greeve, J. (1987) *Biopolymers 26*, 1667–1689.

Pai, E. F., Kabsch, W., Krengel, U., Holmes, K. C., John, J., & Wittinghofer, A. (1989) *Nature 341*, 209–214.

Peticolas, W. L., Kubasek, W. L., Thomas, G. A., & Tsuboi, M. (1987) Raman Spectra and the Conformations of Biological Molecules in *Biological Applications of Raman Spectroscopy* (Spiro, T. G., Ed.) Vol. 1, pp 81–133, John Wiley & Sons, New York.

Schlichting, I., Almo, S. C., Rapp, G., Wilson, K., Petratos, K., Lentfer, A., Wittinghofer, A., Kabsch, W., Pai, E. F., Petsko, G. A., & Goody, R. S. (1990a) *Nature 345*, 309–315.

Schlichting, I., Jacob, J., Frech, M., Chardin, P., Wittinghofer, A., Zimmermann, H., & Rosch, P. (1990b) *Biochemistry 29*, 504–511.

Shelton, K. R., & Clark, J. M. (1967) *Biochemistry 6*, 2735–2739.

Small, E. W., & Peticolas, W. L. (1971) *Biopolymers 10*, 1377–1416.

Spiro, T. G., Ed. (1987) *Biological Applications of Raman Spectroscopy*, Vol. 2, pp 1–367, John Wiley & Sons, New York.

Spiro, T. G., Ed. (1988) *Biological Applications of Raman Spectroscopy*, Vol. 3, pp 1–565, John Wiley & Sons, New York.

Thomas, J. G., & Prescott, B. (1976) *J. Mol. Biol. 102*, 103–124.

Thomas, J. G., & Prescott, B. (1983) *J. Mol. Biol. 165*, 321–356.

Trahey, M., & McCormick, F. (1987) *Science 238*, 542–545.

Tsang, P., Vold, R. R., & Vold, R. L. (1987) *J. Magn. Reson. 71*, 276–282.

Tsuboi, M., Takahashi, S., & Harada, I. (1973) in *Physico-Chemical Properties of Nucleic Acids* (Ducnesne, J., Ed.)

pp 91–145, Academic Press, New York.
Tsuboi, M., Nishimura, Y., Hirakawa, A. Y., & Peticolas, W. L. (1987) in *Biological Applications of Raman Spectroscopy* (Spiro, T. G., Ed.) John Wiley & Sons, New York.
Tucker, J., Sczakiel, G., Feurstein, J., John, J., Goody, R. S., & Wittinghofer, A. (1986) *EMBO J. 5*, 1351–1358.
Wittinghofer, A., Warren, W. F., & Leberman, R. (1977) *FEBS Lett. 75*, 241–243.
Wooley, P., & Clark, B. F. C. (1989) *Bio/Technology 7*, 913–920.
Yue, K. T., Yang, J. P., Charlotte, M., Lee, S. L., Sloan, D., & Callender, R. (1984) *Biochemistry 23*, 6480–6483.
Yue, K. T., Deng, H., & Callender, R. (1989) *J. Raman Spectrosc. 20*, 541–546.
Yue, K. T., Yang, J. P., Charlotte, M., Lee, S. K., Sloan, D., & Callender, R. (1984) *Biochemistry 23*, 6480–6483.

RNA Folding during Transcription by T7 RNA Polymerase Analyzed Using the Self-Cleaving Transcript Assay†

Kamala Tyagarajan, Joseph A. Monforte, and John E. Hearst*

Department of Chemistry, University of California, Berkeley, and Laboratory of Chemical Biodynamics, Lawrence Berkeley Laboratories, Berkeley, California 94720

Received July 3, 1991; Revised Manuscript Received August 27, 1991

ABSTRACT: We have used a self-cleaving RNA molecule (a "hammerhead") to study the length-dependent folding of RNA produced during transcription by T7 RNA polymerase. Transcript elongation is arrested at defined positions using chain-terminating ribonucleoside triphosphate analogues, 3′-deoxynucleoside triphosphates. When the nascent transcript attains the minimum length required for the "hammerhead" domain of the transcript to fully emerge from the ternary complex, the "hammerhead" structure forms and self-cleaves, producing a truncated product. The experiment yields an RNA sequencing ladder which terminates at the length at which cleavage becomes possible; the sequencing ladder is compared to that generated by using a noncleaving control template. We have shown that 13 nucleotides past the cleavage point must be synthesized before the transcript can self-cleave in the ternary complex whereas RNA freed from the complex by heating can cleave with only 3 or more nucleotides present beyond the cleavage site. The results indicate that the RNA in T7 RNA polymerase is not free of steric interactions in the ternary complex and not available for structure formation until it is at least 10 bases away from the site of polymerization. The results suggest that the maximum possible length of the RNA–DNA hybrid in the ternary complexes is 10. The relevance of the results in comparisons with other RNA polymerases, especially *Escherichia coli* RNA polymerase, is discussed.

T7 RNA polymerase is a small, monomeric bacteriophage enzyme with a molecular weight of about 100 000 which is highly specific for the transcription of its well-conserved promoters (Chamberlin & Ryan, 1982). T7 RNA polymerase shares homology with T3, SP6, and yeast mitochondrial RNA polymerases (Masters et al., 1987). In contrast to the larger, multiple-subunit bacterial and eukaryotic RNA polymerases, T7 RNA polymerase is much less complex both structurally and functionally and carries out all the steps of transcription by itself in vitro without the aid of additional protein factors (Coleman, 1974). These components combine to make T7 RNA polymerase an ideal system in which to study the "minimum apparatus" for transcription.

Our studies concern the structure and dynamics of the T7 RNA polymerase·RNA·DNA ternary complex during the elongation phase of transcription. Our experiments address the question of when the nascent RNA transcript becomes free of steric interactions in the ternary elongation complex and is available to form structure with itself. This focus allows us to estimate the maximum possible length of the RNA–DNA hybrid in the ternary elongation complex. It also provides information about the importance of RNA structure formation in processes of pausing and termination which require RNA structure to form within a few nucleotides of the site of polymerization (von Hippel et al., 1984; Yager & von Hippel, 1991).

Footprinting studies have established that between 13 and 19 nucleotides of the DNA are protected by T7 RNA polymerase during elongation (Shi et al., 1988). This establishes an upper limit to the size of the RNA–DNA hybrid. The size of the unwound region of the DNA in the *Escherichia coli* RNA polymerase ternary complex is 17 nucleotides, and the length of the RNA–DNA hybrid is 12 nucleotides (Gamper & Hearst, 1982; Hanna & Meares, 1983; Monforte et al., 1990). Because T7 RNA polymerase is a smaller and simpler enzyme than *E. coli* RNA polymerase, one would expect that the maximum size of the RNA–DNA hybrid in the ternary complex would be either the same or smaller.

Several groups have examined the contacts and accessibility of the nascent RNA chain in order to determine the length of the RNA–DNA hybrid. Hanna and Meares (1983) have used cleavable photoaffinity labeling techniques to show that

† This work was supported by NIH Grant GM41911 to J.E.H. and by Contract DE-AC03-76SF00098 from the Director, Office of Energy Research, Office of General Life Sciences, Structural Biology Division of the U.S. Department of Energy.

* To whom correspondence should be addressed at the Department of Chemistry, Hearst Research Group, University of California, Berkeley.

0006-2960/91/0430-10920$02.50/0